Appl Phys B (2011) 103:653–657
DOI 10.1007/s00340-011-4441-3

Applied Physics B
Lasers and Optics

Optical beam induced current microscopy of photonic quantum ring lasers

R. Hristu · S.G. Stanciu · S.J. Wu · F.-J. Kao · O'D. Kwon · G.A. Stanciu

Received: 23 July 2010 / Revised version: 7 January 2011 / Published online: 1 March 2011

Abstract A confocal laser scanning microscope modified to acquire optical beam induced current images is used to investigate a novel type of semiconductor lasers—photonic quantum ring lasers. We compare the lasing and the photoinduced current images of the structures and analyze their behavior when changing the excitation wavelength. We report the optimal excitation conditions in terms of excitation laser wavelength for collecting the highest photocurrent signal and hence highlighting the photonic quantum ring behavior of the lasers.

1 Introduction

Over the last years an intensive development in the field of semiconductor lasers for low power applications could be observed. Among these devices we can find the whispering gallery modes lasers with submilliampere threshold currents such as the photonic quantum ring (PQR) lasers [1]. These devices, with a structure similar to the cylindrical vertical-cavity surface-emitting lasers (VCSELs), exhibit a two threshold-behavior of successive lasings, first the PQR mode at low currents (μA threshold currents) with the structure lasing on its circumference and then the usual VCSEL mode [2], which occurs for currents in the range of mA. In a PQR laser structure the photons generated in the active region are near-perfectly vertically confined by the top and bottom distributed Bragg reflectors (DBRs). In addition to this vertical confinement, an in-plane annular confinement occurs due to total internal reflection along the lateral boundaries of the active disk as in a microdisk laser, taking place due to the large difference between the refractive index of the active region and that of the covering region.

The 3D confinement of photons generates a toroid effectively formed along the circumference of the active region, without any intentionally fabricated ring structure, the PQR lasing occurring in this region.

In addition to the μA threshold current, the PQR mode has other properties such as a spectral $\sqrt{T}$ dependence and angle-dependent multiple-wavelength radial emission, which make the PQR laser a versatile device for different optoelectronic applications.

These novel photonic devices need non-destructive optical and electrical investigation techniques in order to be characterized with good spatial resolution. One of these techniques is Optical Beam Induced Current (OBIC) microscopy which represents a wide-spread method with applications for the characterization of many semiconductor and optoelectronic devices. It has been previously shown that photocurrent imaging is more sensitive and specific than photoluminescence (PL) imaging in characterizing LEDs [3, 4]. OBIC has also been used to characterize diodes and determine carrier lifetime [5] and also to estimate the diffusion length of carriers in photovoltaic devices [6]. Other investigations have been performed as well using OBIC on photonic devices: uniformity and quantum efficiency of

R. Hristu (✉) · S.G. Stanciu · G.A. Stanciu
Center for Microscopy-Microanalysis and Information Processing, University Politehnica Bucharest, 313 Splaiul Independentei Street, sect. 6, Bucharest, Romania
e-mail: hristu_radu@yahoo.com
Fax: +40-21-4029110

S.J. Wu · F.-J. Kao
Institute of Biophotonics, National Yang-Ming University, Taipei 11221, Taiwan

O'D. Kwon
Department of Electrical Engineering, POTECH—Pohang University of Science and Technology, Pohang 790-784, Republic of Korea

the active region in laser diodes [7, 8], characterization of VCSELs [9].

The OBIC techniques split into various categories such as 1photon(1p)-, 2photon(2p)- [10], and radio frequency (RF) OBIC [11], which have been developed over the years and used to study the dynamics of photo-induced carriers.

The working principle for 1p-OBIC imaging involves a laser source being focused onto the sample by using an objective lens and scanning the laser beam over the sample. If the photon energy is larger than the band-gap of the semiconductor, electron-hole pairs are generated. When electron-hole pairs are created in the neutral region, they will recombine in within the distance of the diffusion length. However when created in the space charge region, they are immediately separated by the electric field and collected by the electrodes to form a current that can be measured. The variations in current flow generated by scanning the laser over the sample are converted in contrast variation and thus constructing the OBIC image.

In this study we show that 1p-OBIC technique represents a suitable investigation method for the characterization of these novel PQR lasers. We have previously reported results regarding OBIC technique used to investigate the PQR structures when employing a HeNe laser with a 633 nm wavelength [12]. Starting from a comparison between the OBIC and electroluminescence (EL) images we show that the properties of the active layer in the PQR circumferential region can be investigated from both the EL and OBIC images. Additionally, the dependence of the photoinduced current with the excitation wavelength highligths a VCSEL-like behavior of the central region different from the behavior of the circumferential region. An advantage of OBIC is that starting from the photocurrent spectrum an excitation wavelength can be selected. Using this wavelength the influence of the central region of the device on the peripheral ring in the OBIC image can be minimized and the ring can be clearly investigated.

2 Experimental

PQR devices of various diameters were investigated using OBIC and EL images.

The PQR structure (Fig. 1) was fabricated on a n-type (100) GaAs substrate grown by metal-organic vapor-phase epitaxy method. The structure consists of two DBR mirrors surrounding a one-λ cavity, which has three 8 nm GaAs quantum wells (QWs), $Al_{0.3}Ga_{0.7}As$ barriers and spacers. The thickness of one-λ cavity is 269.4 nm. There are 38.5 periods in the n-type bottom mirror and 21.5 periods in the p-type top mirror. The mirrors consist of alternating 41.98 nm $Al_{0.15}Ga_{0.85}As$ and 48.82 nm $Al_{0.95}Ga_{0.05}As$ layers. Between the layers, a 20 nm thick linearly graded AlGaAs layer was grown. The p- and n-DBR mirrors were doped to a dose $>10^{18}$ cm^{-3} with C and Si, respectively. The well thicknesses and compositions are tuned to yield a resonance wavelength of 850 nm in the vertical direction.

Cylindrical mesas that are 5.5 μm heigh are structured by chemically assisted ion-beam etching and are planarized by polyimide in order to connect a stripe electrode.

More details regarding the fabrication of similar structures can be found in [13, 14].

The OBIC experimental setup (Fig. 2) was developed based on a commercial Olympus FV300 inverted confocal laser scanning microscope (CLSM). This system has the advantage that it can simultaneously obtain EL and OBIC images. EL images were obtained when the PQR lasers were forward biased and the excitation laser power was zero, while the OBIC images were collected when scanning the structures with different excitation wavelengths.

For collecting the OBIC images and OBIC spectrum we employed a mode locked Ti:Sapphire laser (Coherent Mira-900) with tunable output wavelengths from 700 nm to 1000 nm.

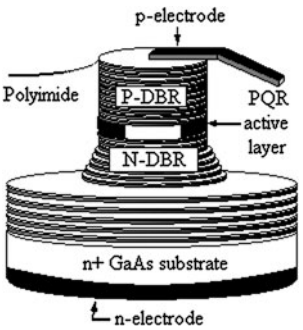

Fig. 1 Diagram of a cylindrical PQR laser structure

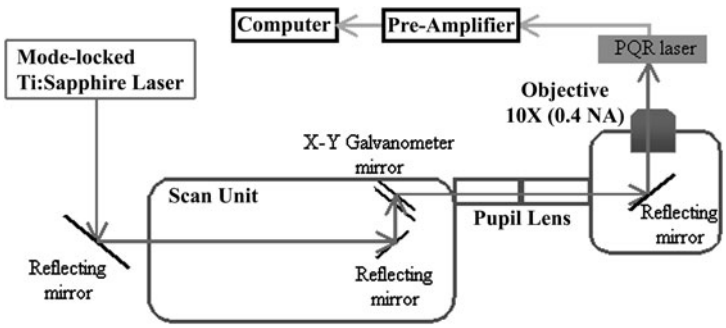

Fig. 2 Experimental setup for OBIC on PQR laser

A 10X 0.4 NA objective was used to optimize the spatial resolution, the field of view and the working distance. A further electronic zoom was used in order to scan only the proximity of the PQR laser structure.

In order to investigate the sample using OBIC technique, the PQR laser is inserted in a usual photodiode connection, with a capacitor used to enable a reduction of the bias supply impedance and a resistor to protect the laser. The resistor value is selected such that the voltage drop caused by the maximum photocurrent is sufficiently smaller than the reverse voltage.

For OBIC imaging, the photocurrent signal (in the range of tens of nA) is pre-conditioned by a current preamplifier (SR-570, Stanford Research) before being fed into the syncronized A/D converter of the CLSM.

In order to evaluate the photocurrent generated by the semiconductor device when scanning the laser over it we have used the freely distributed software application *ImageJ* [http://rsbweb.nih.gov/ij/]. We have averaged the pixels values from the image separately for the central region of the structure and for the surrounding bright ring and got a measure of the generated photocurrent as the intensity in the OBIC image is proportional to the photocurrent. We then normalized the values and ploted them in order to have an estimate on how the device behaves.

3 Results and discussions

Using the setup described in the previous section, EL and OBIC images were acquired (Fig. 3).

The EL image highlights a ring-like lasing on the circumference of the PQR laser as expected. The OBIC image shows the same ring shape pattern on the peripheral region of the laser and an uniform distribution of the photocurrent in the central region. We would like to stress out that if we overlap the EL and OBIC images a strong resemblance between them can be observed, especially when looking at the peripheral ring. Hence, OBIC images show a non-uniform distribution of the photocurrent with a higher intensity on the circumference of the device, proving a different behavior of the peripheral ring-shaped region compared to the central area of the structure, similar to the PQR and VCSEL modes in the EL.

Using the tunability of the Ti:Sapphire laser the dependence between the photoinduced current and the wavelength of the exciting laser is investigated.

For optoelectronic devices in general, the shape of the photocurrent spectrum is closely connected to the absorption of the whole structure. There are also other contributions that should be taken into consideration like those related to defect or impurity absorption [8].

For VCSEL-like structures, PQR lasers included, the influence of the cavity formed by the upper and lower DBRs must additionally be taken into account. Basically, these laser structures are resonant cavities formed between the two DBR mirrors. The mirror pattern affects the entire photocurrent spectrum including the spectrum around the lasing wavelength as well as the spectral region situated below the emission wavelength [9].

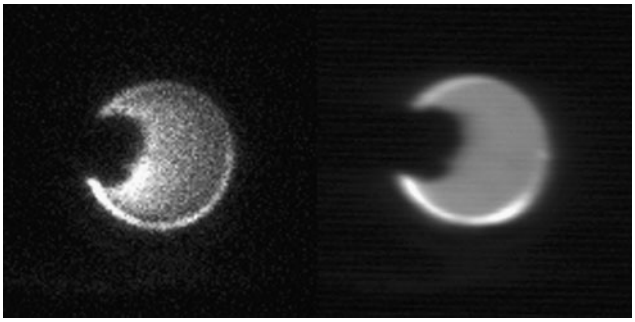

Fig. 3 EL of a 32 μm PQR laser and corresponding OBIC image (excitation wavelength—790 nm)

Looking at the OBIC spectra (Fig. 4) one can identify a different behaviour of the central region as compared to the periphery of the structure.

For the central region of the PQR laser a typical VCSEL behavior [15] can be observed. For wavelengths lower than 710 nm (1.74 eV) the absorption in the upper $Al_{0.3}Ga_{0.7}As$ barrier, with a band-gap energy $E = 1.8$ eV, influences the OBIC spectrum. Starting with 750 nm the influence of the upper and lower DBR mirrors on the OBIC spectrum is higher. The photocurrent peaks outside the DBR mirror stop band at $\lambda = 760$ nm, $\lambda = 780$ nm and $\lambda = 795$ nm are due to transmission maxima of the upper DBR. The peak at $\lambda = 760$ nm (1.63 eV) can also be due to the absorption within the $Al_{0.15}Ga_{0.85}As$ layer in the upper DBR that has a band-gap energy $E = 1.61$ eV. The main photocurrent feature at 837 nm is in good correspondence with the measured emission wavelength of the device at 835 nm and spectrally lies in the reflectance stop band of the resonant cavity that extends from 805 nm to over 850 nm, beyond our measured range.

The OBIC spectrum for the peripheral ring is constantly decreasing from 700 nm to 810 nm due to the decrease in absorption, same as in the case of a multiple quantum well structure [16]. The influence of the DBR mirror and resonant cavity to the spectrum is minimal, being visible between 760 nm and 800 nm where the spectrum slightly increases similar to the OBIC spectrum for the central region. At wavelengths close to the emission wavelength (835 nm) the dominant excitonic contribution to the GaAs band-edge absorption is visible. It is slightly moved to higher energies than the bulk GaAs band-gap energy (1.42 eV) due to the quantum well effect. When the excitation wavelength is higher than the emission wavelength, the OBIC spectrum drops to zero.

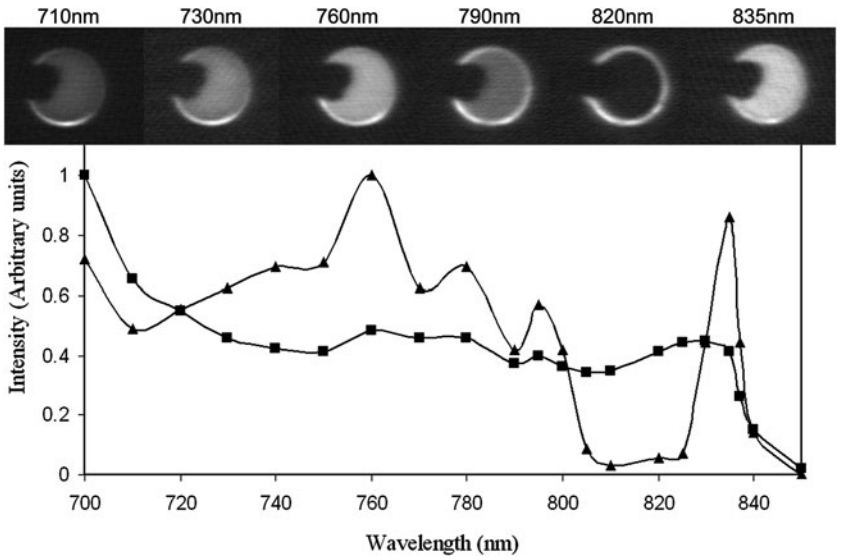

Fig. 4 OBIC spectrum for the ring (*squares*) compared to the spectrum for the central region of the PQR laser (*triangles*). The inset is a series of OBIC images from a 32 μm diameter PQR laser with the corresponding excitation wavelengths

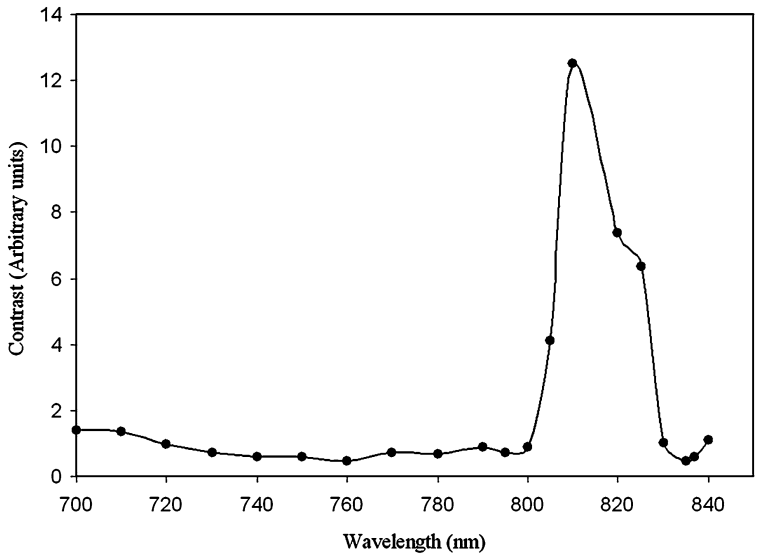

Fig. 5 Contrast ratio between the central region and the peripheral ring

The advantage of the OBIC technique is that when using a tunable laser one can choose an excitation wavelength that is most suited for the experiment.

The importance of a tunable wavelength excitation laser source for optimum confocal OBIC was previously analysed [4]. It is crucial to use a tunable source in order to match the excitation wavelength to the properties of the sample under investigation, such as emission wavelength or some features to be characterized. In the case of PQR lasers this wavelength would be that which offers the best contrast between the central region and the ring in the OBIC spectrum, in order to highligth the peripheral ring.

The ideal case would be to find an excitation wavelength that would allow photocurrent generation only from the PQR peripheral region, hence offering a good characterization method for the PQR behavior of the device. Because of the VCSEL-like behavior of the central region and the high OBIC response, the influence on the peripheral ring is high. Best results would be achieved by using a wavelength for which the contrast ratio between the response of the two regions would be as high as possible.

Considering the contrast between the peripheral ring and the central region (Fig. 5) and also the OBIC spectrum of the two areas, one can observe that between 750 nm and 800 nm the influence of the central region on the peripheral ring is pronounced, as mentioned earlier. Looking in the spectral region corresponding to the stop band of the resonant cavity, between 800 nm and 825 nm, the contrast is higher because the reflectivity of the upper DBR is high and the OBIC generated in the central region is low. Additionally, the lowest possible wavelength would be preferred, as it has a lower penetration depth and carriers generated in the central region will not be in the vicinity of the active area, hence a smaller photocurrent originating from the central region.

Fig. 6 OBIC images of different 32 μm diameter structures (excitation wavelength 810 nm)

Our experiments show that the 810 nm wavelength can be regarded as the best one for investigations on PQR lasers, because it is the smallest wavelength in the stop band and also offers good results in terms of contrast in the OBIC images (Fig. 6).

Due to the non-uniform distribution of the photocurrent and the higher intensity on the periphery of the structure and also because the photocurrent strongly depends on the excitation wavelength, choosing the right wavelength is very important in investigating the PQR lasers and especially the PQR behavior of the structures.

4 Conclusions

We have investigated PQR lasers using the OBIC technique. We have shown that OBIC can be used to investigate these structures proving a VCSEL-like behavior of the central region different from the behavior of the peripheral ring that correspond to the PQR lasing in EL images. Using the tunable Ti:Sapphire laser we have found a suitable wavelength close to the emission wavelength of the PQR laser. When using this excitation wavelength the best contrast between the photocurrent generated in the central region and the photocurrent from the peripheral ring can be achieved and investigations on the peripheral ring can be performed with the unwanted influence of the central part of the laser minimized. This technique can be applied to investigate the PQR behavior of these laser devices.

Acknowledgements This work was supported by CNCSIS–UEFISCDI, project number PNII–IDEI 1566/2008, contract number 726/2009.

References

1. J.C. Ahn, H.Y. Kang, O'D. Kwon, Proc. SPIE **3283**, 241 (1998)
2. J.C. Ahn, K.S. Kwak, B.H. Park, H.Y. Kang, J.Y. Kim, O'D. Kwon, Phys. Rev. Lett. **82**, 536 (1999)
3. F.J. Kao, M.K. Huang, Y.S. Wang, S.L. Huang, M.K. Lee, C.K. Sun, Opt. Lett. **24**, 1407 (1999)
4. E. Esposito, F.-J. Kao, G. McConnell, Appl. Phys. B **88**, 551 (2007)
5. C. Raynaud, S.-R. Wang, D. Planson, M. Lazar, J.-P. Chante, Diam. Relat. Mater. **13**, 1697 (2004)
6. Y. Sayad, A. Kaminski, D. Blanc, A. Nouiri, M. Lemiti, Superlattices Microstruct. **45**, 393 (2009)
7. G. Stanciu, D. Botez, Microsc. Anal. **88**, 5 (2002)
8. A. Richter, J.W. Tomm, Ch. Lienau, J. Luft, Appl. Phys. Lett. **69**, 3981 (1996)
9. J.W. Tomm, T. Gunther, Ch. Lienau, A. Gerhardt, J. Donecker, J. Cryst. Growth **210**, 296 (2000)
10. C. Xu, W. Denk, J. Appl. Phys. **86**, 2226 (1999)
11. F.J. Kao, J.C. Chen, S.C. Shih, A. Wei, S.L. Huang, T.S. Horng, P. Török, Opt. Commun. **211**, 39 (2002)
12. G.A. Stanciu, S.G. Stanciu, R. Hristu, D.K. Kim, O'D. Kwon, in *Proc. of the ICTON 2008*, Marakech, 11–13 Dec. (2008)
13. J.Y. Kim, K.Y. Kwak, J.S. Kim, B. Kang, O'D. Kwon, J. Vac. Sci. Technol. B **19**, 1334 (2001)
14. J.C. Ahn, H.Y. Kang, N.J. Son, B.H. Park, K.S. Kwak, Y.H. Lee, O'D. Kwon, Jpn. J. Appl. Phys. **36**, 2134 (1997)
15. A. Jaeger, P.M. Petroff, T.D. Lowes, Appl. Phys. Lett. **78**, 3012 (2001)
16. M. Bugajski, K. Reginski, Opto-Electron. Rev. **4**, 83 (1996)